

---

---

# The Prognostic Value of Quantitative Bone SPECT/CT Before $^{223}\text{Ra}$ Treatment in Metastatic Castration-Resistant Prostate Cancer

Helmut Dittmann<sup>1</sup>, Sabine Kaltenbach<sup>1</sup>, Matthias Weissinger<sup>1</sup>, Francesco Fiz<sup>1</sup>, Peter Martus<sup>2</sup>, Maren Pritzkow<sup>1</sup>, Juergen Kupferschlaeger<sup>1</sup>, and Christian la Fougère<sup>1,3</sup>

<sup>1</sup>Department of Nuclear Medicine and Clinical Molecular Imaging, University Hospital Tuebingen, Tuebingen, Germany; <sup>2</sup>Institute for Clinical Epidemiology and Applied Biometry, University of Tuebingen, Tuebingen, Germany; and <sup>3</sup>iFIT Cluster of Excellence, University of Tuebingen, Tuebingen, Germany

---

Radiolabeled bisphosphonates such as  $^{99\text{m}}\text{Tc}$ -3,3-diphosphono-1,2-propanodicarboxylic acid ( $^{99\text{m}}\text{Tc}$ -DPD) typically show intense uptake in skeletal metastases from metastatic castration-resistant prostate cancer (mCRPC). Extensive bone involvement is regarded as a risk factor for mCRPC patients treated with  $^{223}\text{Ra}$ -dichloride ( $^{223}\text{Ra}$ ). The aim of this study was to quantify  $^{99\text{m}}\text{Tc}$ -DPD uptake by means of SPECT/CT before  $^{223}\text{Ra}$  and compare the results with the feasibility of treatment and overall survival (OS). **Methods:** Sixty consecutive mCRPC patients were prospectively included in this study. SPECT/CT of the central skeleton covering the skull to the mid-femoral level was performed before the first cycle of  $^{223}\text{Ra}$ . The bone compartment was defined by means of low-dose CT. Emission data were corrected for scatter, attenuation, and decay supplemented by resolution recovery using dedicated software. The Kaplan-Meier estimator, *U* test, and Cox regression analysis were used for statistics. **Results:** Total  $^{99\text{m}}\text{Tc}$ -DPD uptake of the central skeleton varied between 11% and 56% of injected dose (%ID) or between 1.8 and 10.5 %ID/1,000 mL of bone volume (%ID/L).  $\text{SUV}_{\text{mean}}$  ranged from 1.9 to 7.4, whereas the  $\text{SUV}_{\text{max}}$  range was 18–248. Patients unable to complete  $^{223}\text{Ra}$  treatment because of progression and/or cytopenia ( $n = 23$ ) showed significantly higher uptake (31.9 vs. 25.4 %ID and 6.0 vs. 4.7 %ID/L;  $P < 0.02$ ). OS after  $^{223}\text{Ra}$  (median, 15.2 mo) was reduced to 7.3 mo in cases of skeletal uptake that was 26 %ID or higher, as compared with 30.8 mo if lower than 26 %ID ( $P = 0.008$ ). Similar results were obtained for %ID/L and  $\text{SUV}_{\text{mean}}$ .  $\text{SUV}_{\text{max}}$  did not correlate with survival. %ID/L was identified as an independent prognostic factor for OS (hazard ratio, 1.381 per unit), along with number of previous treatment lines. **Conclusion:** Quantitative SPECT/CT of bone scans performed at baseline is prognostic for survival in mCRPC patients treated with  $^{223}\text{Ra}$ .

**Key Words:** SPECT/CT; quantification; prostate cancer; bone scan;  $^{223}\text{Ra}$

**J Nucl Med 2021; 62:48–54**

DOI: 10.2967/jnumed.119.240408

**M**etastatic castration-resistant prostate cancer (mCRPC) is a bone-dominant disease, with about 90% of patients affected by osseous involvement (1). Skeletal metastases are a major threat to patient quality of life because they cause pain, pathologic fractures, and neurologic dysfunction. Depletion of the hematopoietic marrow by tumor expansion is recognized as the major cause of cancer-specific death in mCRPC (2). To overcome this problem, various new treatments have been developed, including novel radiopharmaceuticals (3,4).

Bone scintigraphy using  $^{99\text{m}}\text{Tc}$ -labeled bisphosphonates is still considered the standard of choice for imaging of bone metastases in mCRPC (5). With the introduction of SPECT/CT, sensitivity and diagnostic accuracy have been considerably improved as compared with 2-dimensional imaging (6). The extent of bone involvement is usually reported by applying qualitative or semiquantitative measures such as the number of lesions. PET/CT with  $\text{Na}^{18}\text{F}$  is an alternative to bone scintigraphy that comes with superior image resolution and allows for absolute quantification (7). However,  $\text{Na}^{18}\text{F}$  PET/CT suffers from limited availability and thus has not yet been recommended by guidelines (8). Moreover, it lacks reimbursement in most countries.

Osteotropic radiopharmaceuticals also allow for targeted irradiation following a theranostic approach (9). The  $\alpha$ -emitter  $^{223}\text{Ra}$ -dichloride ( $^{223}\text{Ra}$ ) was shown to improve overall survival (OS) in mCRPC (10) and reduce skeleton-related events at favorable tolerability (11). Conversely, the optimal role of  $^{223}\text{Ra}$  in the growing instrumentarium against mCRPC has yet to be defined (12,13).

Earlier work has demonstrated that a high extent of bone involvement as identified by bone scans is a risk factor for patients with mCRPC. In the pivotal  $^{223}\text{Ra}$  trial, a large number of skeletal lesions was associated with an elevated risk for cytopenia (14). Although the rate of anemia was comparable between the  $^{223}\text{Ra}$  and placebo groups, thrombocytopenia was more frequent in the  $^{223}\text{Ra}$  group. High osseous tumor load as measured by  $\text{Na}^{18}\text{F}$  PET/CT was shown to be associated with poor OS after  $^{223}\text{Ra}$  (15). More recently, semiautomated estimation of bone metastatic involvement, creating a bone scan index, has been shown to be related to poor survival in patients with great tumor burden (16,17). Since that approach involves only planar images, the projected 2-dimensional anatomy may be subject to summation artifacts (18). As a result, differentiation of metastases from normal bone can be challenging in advanced tumor spread, and a bone scan index might not be obtainable for all

---

Received Dec. 3, 2019; revision accepted Apr. 22, 2020.  
For correspondence or reprints contact: Helmut Dittmann, University Hospital Tuebingen, Otfried-Mueller-Strasse 14, Tuebingen, D-72076, Germany.  
E-mail: helmut.dittmann@med.uni-tuebingen.de  
Published online May 22, 2020.  
COPYRIGHT © 2021 by the Society of Nuclear Medicine and Molecular Imaging.

patients (17). Delineation of metastatic tumor load would be especially difficult in the case of a superscan finding (19).

Recent development has allowed for quantification of SPECT/CT data similar to PET/CT (20,21). Here, we report on quantitative bone SPECT/CT to analyze bisphosphonate uptake of the central skeleton. This approach is based on the notion that the higher the overall bone uptake is, the higher is the osteoblastic tumor load. We hypothesize that the resulting measure of bone metabolism may be prognostic in patients treated with  $^{223}\text{Ra}$ . A prospective clinical study was conceived, aiming to evaluate whether the results of quantitative bone scan imaging correlate with completion of the subsequent  $^{223}\text{Ra}$  treatment course and survival.

## MATERIALS AND METHODS

### Patient Population

This prospective, observational study included mCRPC patients with symptomatic osseous metastases referred to our institution for  $^{223}\text{Ra}$  treatment. A bone scan including quantitative SPECT/CT was planned for all individuals lacking a recent pretest ( $\leq 2$  mo before the planned treatment). CT or MRI scans of the thorax, abdomen, and pelvis were obtained to evaluate visceral and lymph node involvement. Patients with lymph node metastases up to a maximum diameter of 3 cm were accepted, whereas patients with visceral metastasis were excluded. This study was conceived as part of an extensive clinical protocol on SPECT/CT quantification registered in the German Registry for Clinical Studies (DRKS00013571) (22). The study was approved by the institutional review board (decision 747/2014BO1), and all subjects gave written informed consent.

### $^{223}\text{Ra}$ Treatment

$^{223}\text{Ra}$  treatment was scheduled as a series of 6 cycles at 4-wk intervals, with dose adapted to body weight (55 kBq/kg). In cases of cytopenia, subsequent cycles could be postponed up to week 8 from the previous dose to allow for recovery.  $^{223}\text{Ra}$  treatment was considered completed in patients who received 5–6 cycles. Serum prostate-specific antigen level and blood cell counts were collected at baseline, and blood cell counts were recorded approximately every 2 wk during treatment. Cytopenia was classified according to the Common Terminology Criteria for Adverse Events (CTCAE), version 4.03 (23). Since osseous progression and treatment-related hematotoxicity may lead to reduced blood cell numbers, distinction between these causes can be challenging or even impossible in individual cases. In practice, decreased blood cell levels are often caused by a combination of both. In this study, we report as cytopenia any reduction in blood cell elements corresponding to CTCAE grade 2 or higher, irrespective of its possible cause.

### Bone Imaging

Imaging was performed within 30 d before the first cycle of  $^{223}\text{Ra}$ . Patients received, on average,  $632 \pm 56$  MBq of  $^{99\text{m}}\text{Tc}$ -3,3-diphosphono-1,2-propanodicarboxylic acid ( $^{99\text{m}}\text{Tc}$ -DPD) (CIS Bio International) intravenously. A dual-detector SPECT/CT camera (Discovery NM/CT 670 Pro; GE Healthcare) was used throughout. Approximately 3 h from  $^{99\text{m}}\text{Tc}$ -DPD injection, planar images of the whole body were acquired in anterior and posterior views (table feed, 15 cm/min of acquisition;  $1,028 \times 256$  matrix) followed by SPECT/CT. For the SPECT acquisition, the camera heads were in H-mode. There were 3 fields of view covering the skull to the mid-femoral level, with the arms adducted laterally to the body. The matrix was  $128 \times 128$  matrix. Thirty steps were used, with a 15-s acquisition per step. Images were reconstructed using iterative ordered-subset expectation maximization (4 iterations and 10 subsets) without pre- or postfiltering. Then, a non-contrast-enhanced CT scan (dose-length product, 358–462 mGy-cm; 120 kV; slice thickness, 2.5 mm) was obtained for attenuation correction and anatomic mapping.

Finally, the reconstructed SPECT data were coregistered with the CT images on a dedicated workstation (Xeleris 4; GE Healthcare). The images were read by 2 experienced nuclear medicine specialists. On planar whole-body images, focal areas of increased uptake suggestive of osseous metastasis were recorded and classified as fewer than 6 lesions, 6–20, more than 20, or superscan (diffuse, intense skeletal uptake without renal and background radioactivity).

### Quantification

To quantify  $^{99\text{m}}\text{Tc}$ -DPD uptake, tomographic SPECT data were corrected for attenuation, scatter, and resolution recovery using a dedicated software algorithm (Evolution; GE Healthcare). SPECT/CT of a cylindrical phantom (21 cm in diameter and 20 cm in height) filled with  $^{99\text{m}}\text{Tc}$  and water at a known activity concentration was used to calculate system sensitivity. This procedure was repeated after each system calibration (uniformity, energy, linearity) every 6 mo. In addition, planar sensitivity using a point source was measured weekly to define a reference value (tolerance  $\pm 5\%$ ).

Volumes of interest were defined by means of a proprietary semiautomatic segmentation application (Q.metrix; GE Healthcare). At first, the skeletal bone compartment was delineated using CT-measured density (lower threshold, +200 Hounsfield units). Areas outside the skeletal compartment, such as vessel calcifications, were meticulously reviewed and manually excluded. The resulting volume of interest thus represented the entire central skeleton compartment from the skull to the mid-femoral level. Then, the following measures of tracer uptake in the bone volumes of interest were extracted:

**TABLE 1**  
Baseline Characteristics of Patients

Variable	Data
Age (y)	71 (55–90)
Gleason score	
$\leq 7$	17 (28%)
$\geq 8$	36 (60%)
Unknown	7 (12%)
Prostate-specific antigen level ( $\mu\text{g/L}$ )	65 (1.1–9,375)
Preexisting cytopenia grade 2	7 (12%)
Anemia	5 (8%)
Neutropenia	1
Thrombocytopenia	1
Prior treatment lines for mCRPC	
0	17 (28%)
1	20 (33%)
2	14 (23%)
3 or more	9 (15%)
Prior chemotherapy	26 (43%)
Extent of bone disease	
$< 6$ metastases	4 (7%)
6–20 metastases	17 (28%)
$> 20$ metastases	32 (53%)
Superscan	7 (12%)

Qualitative data are numbers followed by percentages in parentheses; continuous data are median followed by range in parentheses. Percentages may not sum to 100 because of rounding.

**TABLE 2**  
Quantitative SPECT/CT Results for Bone Scans Before  $^{223}\text{Ra}$  Treatment

Parameter	Mean	Median	Range
Skeletal volume (mL)	5,447	5,491	4,161–7,720
%ID	27.8	25.7	11–56
%ID/L	5.2	4.5	1.8–10.5
SUV <sub>mean</sub>	4.1	3.9	1.9–7.4
SUV <sub>max</sub>	82.4	70.2	18–248

percentage injected dose (%ID), %ID per 1,000-mL bone volume (%ID/L), SUV<sub>mean</sub>, and the SUV<sub>max</sub> in any of a patient's tumor lesions.

### Statistics

Differences in parameters between patient groups (complete vs. incomplete  $^{223}\text{Ra}$  treatment) were compared using the Mann–Whitney *U* test. The Kaplan–Meier estimator and log rank test were used to assess patients' survival fraction categorized for quantitative SPECT/CT variables. Receiver-operating-characteristic analysis was executed to analyze the performance of SPECT/CT to prognosticate early death and incomplete treatment. Simple and multiple Cox regression proportional-hazards analysis and logistic regression were performed to analyze the influence of variables on OS and treatment completion. Stepwise-forward variable selection was applied with inclusion and exclusion probabilities of 0.05 and 0.10, respectively. All analyses were performed using SPSS software (version 25; IBM). An  $\alpha$ -level of 0.05 (2-sided) was considered significant. No correction for multiple testing was performed.

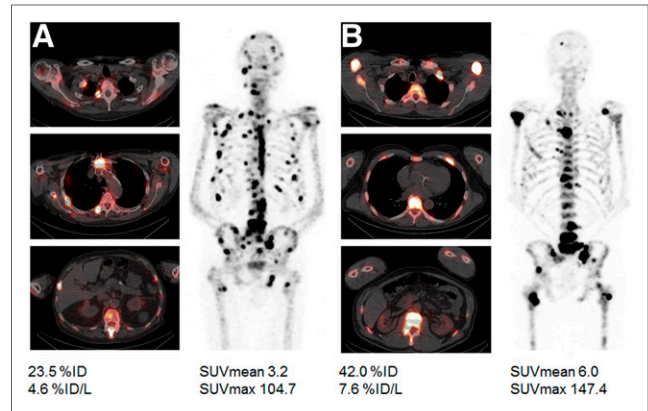


**FIGURE 2.** Typical case studies in 2 patients with disseminated bone metastasis. Quantitative SPECT/CT revealed low to moderate parameters of  $^{99\text{mTc}}$ -DPD uptake except for pronounced SUV<sub>max</sub> in patient A, whereas all measures were markedly high in patient B. Both patients subsequently received 6 cycles of  $^{223}\text{Ra}$ . OS in patient A (85 y old) was 13 mo, whereas patient B (72 y old) survived for only 7 mo after start of  $^{223}\text{Ra}$ .

### RESULTS

#### $^{223}\text{Ra}$ Treatment and Follow-up

From March 2015 until June 2018, 65 consecutive patients fulfilled the inclusion criteria for this study and subsequently received at least one cycle of  $^{223}\text{Ra}$ . Sixty of these individuals could be included. Four patients were excluded because they lacked or had incomplete SPECT/CT data, and one patient was excluded because SPECT/CT could be performed only after the first  $^{223}\text{Ra}$  cycle. The clinical characteristics of the patients are shown in Table 1. The mean follow-up after  $^{223}\text{Ra}$  treatment was 13.6 mo (range, 1–42 mo). Thirty-five patients died during the study period. Median OS since the first  $^{223}\text{Ra}$  therapy cycle was 15.2 mo. Moderately decreased blood cell counts corresponding to CTCAE grade 2 were present in 7 patients before  $^{223}\text{Ra}$  (Table 1), whereas most patients had no relevant myelosuppression. New-onset cytopenia of CTCAE grades 2–4 was observed in 21 of 53 patients (38.6%; 95% CI, 26.5%–54.0%) during  $^{223}\text{Ra}$ . Severe myelosuppression, grades 3–4, developed in 10 patients ( $n = 9$  newly evolved [6 anemias, 0 thrombocytopenia, 2 neutropenias, 1 leukopenia];  $n = 1$  aggravation of preexisting bicytopenia in erythrocytes and platelets [17%; 95% CI, 8.1–29.9]). The scheduled  $^{223}\text{Ra}$  course could be completed in 36 of 60 individuals, with 279 cycles applied in total (6 cycles,  $n = 36$ ; 4 cycles,  $n = 6$ ; 3 cycles,  $n = 7$ ; 2 cycles,  $n = 7$ ; 1 cycle,  $n = 4$ ). Reasons for early termination (prevalence, 40%; 95% CI, 27.6%–53.5%) were tumor progression ( $n = 15$ ), cytopenia of grade 3 or 4 ( $n = 5$ ), or a combination of both ( $n = 3$ ). In one patient without evidence of myelosuppression or progression,  $^{223}\text{Ra}$  was terminated after 4 cycles following a novel reported contraindication against the combination of  $^{223}\text{Ra}$  with

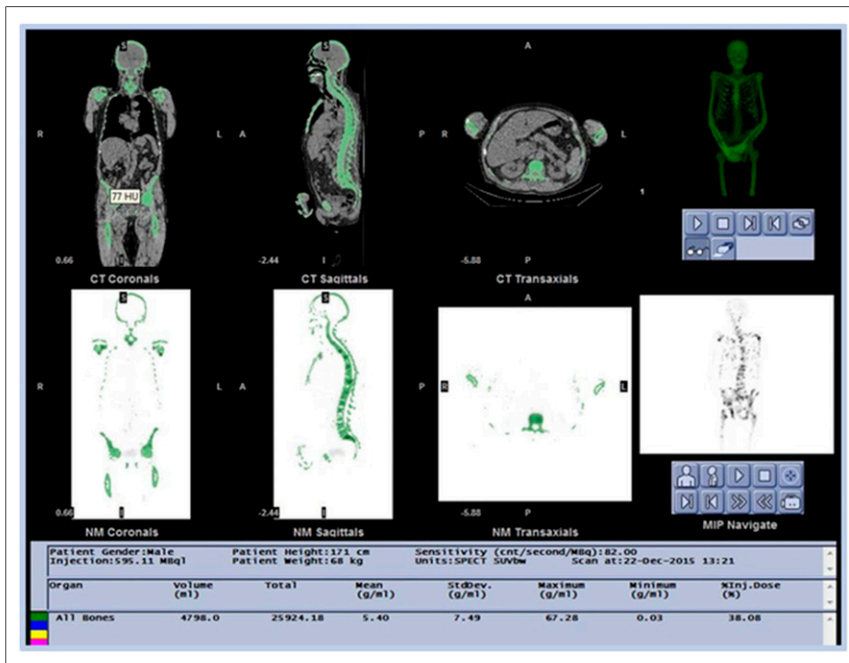


**FIGURE 1.** Bone compartment as defined by CT and quantitative data for  $^{99\text{mTc}}$ -DPD uptake in a mCRPC patient with osseous metastases. The image shows a screenshot of the output generated using the semiautomatic segmentation application. Images show central coronal, sagittal, and transaxial CT slices (upper row) and SPECT slices (lower row) with superposed bone compartment VOI (green). cnt = counts; NM = nuclear medicine; MIP = maximum-intensity projection; SUVbw = SUV normalized to patient body weight.

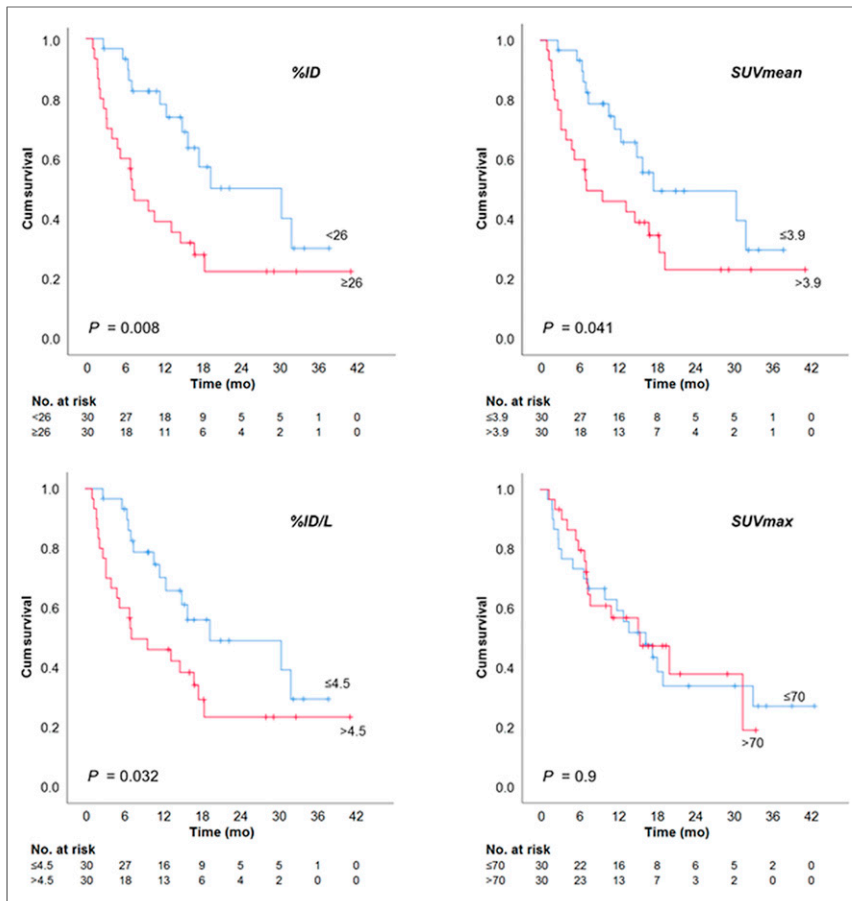


**FIGURE 3.** Kaplan–Meier analysis of OS since start of  $^{223}\text{Ra}$  treatment, stratified for quantitative SPECT/CT measures of  $^{99\text{m}}\text{Tc}$ -DPD uptake. Cum = cumulative.

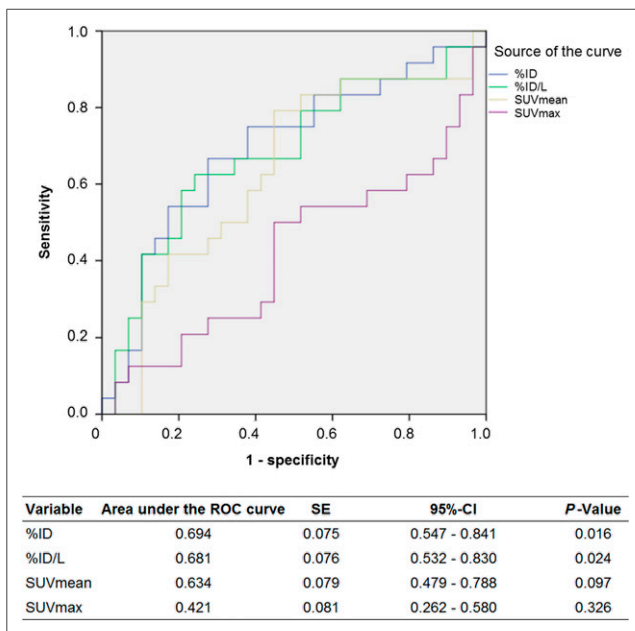


**FIGURE 4.** Receiver-operating-characteristic (ROC) analyses showing sensitivity and specificity of quantitative SPECT/CT variables in prognosticating death within first year after  $^{223}\text{Ra}$ . CI = confidence interval.

abiraterone and prednisolone. This case was excluded from analyses stratified for completed versus incomplete  $^{223}\text{Ra}$  treatment. In total, 13 patients continued abiraterone or enzalutamide under  $^{223}\text{Ra}$  before the contraindication for combination treatment was reported in November 2017. No patient received  $^{223}\text{Ra}$  combined with novel antiandrogens during the remaining study period. Two patients developed pathologic fractures during  $^{223}\text{Ra}$  treatment (1 on  $^{223}\text{Ra}$  monotherapy, 1 on  $^{223}\text{Ra}$  plus abiraterone), both of which were assigned to additional external-beam irradiation before  $^{223}\text{Ra}$  was resumed.

### Quantitative $^{99\text{m}}\text{Tc}$ -DPD Uptake as Prognosticator of Survival

Planar whole-body scans revealed increased uptake in osseous metastases in all cases. Most scans visualized multiple bone lesions with increased tracer uptake, classified as either more than 20 lesions or superscan in about two thirds of patients (Table 1). Quantification showed a mean total  $^{99\text{m}}\text{Tc}$ -DPD uptake of 27.8 %ID in the central skeleton, or 5.2 %ID/L (Table 2), with considerable variance between individuals. The mean  $^{99\text{m}}\text{Tc}$ -DPD uptake was calculated to have an  $\text{SUV}_{\text{mean}}$  of 4.1. Tumoral  $\text{SUV}_{\text{max}}$  showed particularly high variability in our patient cohort. Typical clinical examples are shown in Figures 1 and 2.

Kaplan–Meier analyses with thresholds set to median revealed a significantly shortened OS of 7.3 mo in patients with at least 26 %ID or more than 4.5 %ID/L (Fig. 3). The cohort of individuals with lower total uptake had a favorable survival of 30.8 and 19.6 mo, instead. A similar trend was also seen for  $\text{SUV}_{\text{mean}}$ , with a threshold of 3.9 (7.3 vs. 17.8 mo). In contrast,  $\text{SUV}_{\text{max}}$  was not associated with survival. The 1-y OS rate after the start of  $^{223}\text{Ra}$  was 55% ( $n = 29/53$ , 7 censored). Receiver-operating-characteristic analysis of SPECT/CT variables demonstrated that high %ID and %ID/L were moderately accurate for prognosticating death during the first year (Fig. 4).  $\text{SUV}_{\text{mean}}$  showed only a trend for connection with first-year mortality, whereas  $\text{SUV}_{\text{max}}$  was not linked with early death.

Quantitative SPECT/CT variables and clinical characteristics (age, prostate-specific antigen level, tumor load categories, prior chemotherapy, number of previous treatment lines for mCRPC) were included as candidates in a Cox regression model for prediction of OS. Because prostate-specific antigen level was not distributed normally, decadic logarithm prostate-specific antigen was used instead. At univariate regression analyses, %ID, %ID/L, extent of bone disease, number of previous treatment cycles for mCRPC, and history of chemotherapy were significantly associated with OS. Multiple Cox regression identified %ID/L and the number of previous therapy lines for mCRPC as independent predictors of survival (Table 3).

### Early Termination Versus Completed $^{223}\text{Ra}$ Treatment

Median OS was only 5.8 mo in patients unable to complete the full  $^{223}\text{Ra}$  treatment because of progression and/or cytopenia

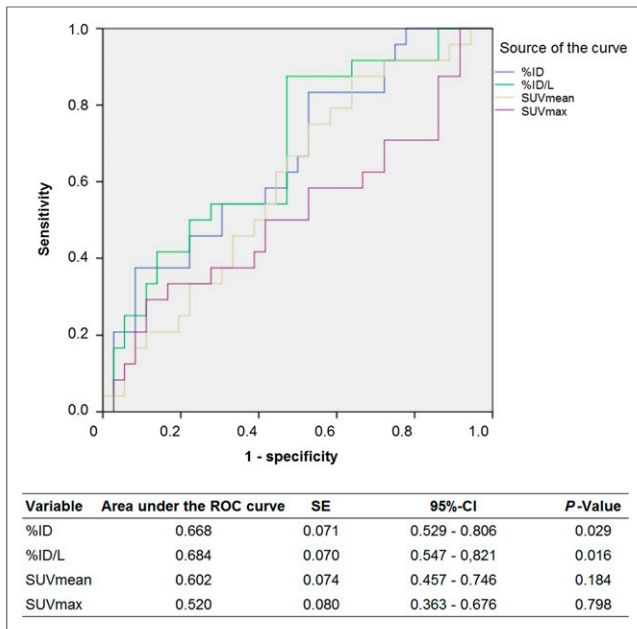


**FIGURE 5.** Receiver-operating-characteristic (ROC) analyses showing sensitivity and specificity of quantitative SPECT/CT variables in prognosticating failure to complete subsequent  $^{223}\text{Ra}$  therapy. CI = confidence interval.

( $n = 23$ ), whereas patients who received the complete course had a median survival of 30.8 mo ( $P < 0.001$ ). Patients with early terminated treatment showed a significantly higher total  $^{99\text{m}}\text{Tc}$ -DPD uptake (mean, 31.9 %ID vs. 25.4 [ $P = 0.017$ ]; %ID/L, 6.0 vs. 4.7 [ $P = 0.014$ ]), whereas SUV<sub>mean</sub> or SUV<sub>max</sub> did not statistically differ between groups. Receiver-operating-characteristic analysis demonstrated an association of %ID and %ID/L with incomplete  $^{223}\text{Ra}$ , though considerable overlap limited discrimination from patients able to receive full treatment (Fig. 5). Univariate regression analysis demonstrated %ID/L and the number of previous treatment lines as predictors of incomplete  $^{223}\text{Ra}$  therapy (Table 4). Multiple logistic regression identified %ID/L as the sole independent predictor of incomplete  $^{223}\text{Ra}$  treatment.

## DISCUSSION

Quantitative measures of bone metastatic disease are desirable for risk stratification in patients considered for  $^{223}\text{Ra}$  treatment. The current prospective study on quantitative bone scan SPECT/CT demonstrated shortened OS for mCRPC patients with high bisphosphonate uptake before  $^{223}\text{Ra}$ . All measures of average bone uptake in the central skeleton (%ID, %ID/L, and SUV<sub>mean</sub>) were associated with survival. In particular, %ID at a threshold of 26 or higher showed the strongest separation of prognostic groups (7.3 mo vs. >30 mo survival). Multiple regression identified %ID/L as an independent prognostic variable of OS along with the number of previous treatment lines. Furthermore, high uptake was associated with inability to complete the planned  $^{223}\text{Ra}$  sequence, due to progression or cytopenia. In fact, %ID/L was the only independent prognosticator of completion failure at multivariate analysis. The observed relations should not lead to denial of  $^{223}\text{Ra}$  treatment, as patients unable to complete the course may still benefit from  $^{223}\text{Ra}$ . Although overlap between prognostic groups may limit the use of quantitation for individual decision making, risk stratification could be helpful for clinical studies on mCRPC treatment. In contrast, SUV<sub>max</sub> of the most intensive lesion seems to be independent of cumulative tumor load. According to Na $^{18}\text{F}$  PET/CT (15) and the current results, SUV<sub>max</sub> did not correlate with survival. Thus, maximum uptake does not seem to be of value for defining a reference lesion that might prognosticate outcome.

Our results correspond to the findings of retrospective studies demonstrating poor survival in patients with an extensive metastatic burden expressed as a bone scan index (17) or high tumor volume estimated by quantitative Na $^{18}\text{F}$  PET/CT (15). Recently, a similar approach has been suggested using quantification by SPECT/CT of bone scans (24). It has also been shown that bisphosphonate uptake as measured by quantitative SPECT/CT closely correlates with that of Na $^{18}\text{F}$  (25). The methodology in the previous studies differed from our approach in that cutoffs, based on either SUV or count rates, were hitherto used to separate metastatic from normal bone so as to define the osseous tumor load. Overlap between uptake of normal and metastatic bone (26) is a potential limitation of cutoffs that may lead to false-positive results. This limitation might be circumvented using a relatively high cutoff, possibly at the price of underestimating tumor volume. In addition, cutoffs will have to be individually established for the scanner used for imaging (27). By

**TABLE 3**  
Cox Proportional Hazards Regression Analysis on Association of Multiple Variables and OS after  $^{223}\text{Ra}$  Treatment

Variable	Univariate regression			Cox multiple regression		
	P	Hazard ratio	95% CI	P	Hazard ratio	95% CI
%ID (per 1 unit)	0.005	1.046	1.014–1.079			
%ID/L(per 1 unit)	0.003	1.259	1.083–1.464	<0.001	1.381	1.162–1.643
SUV <sub>mean</sub> (per 1 unit)	0.068	1.225	0.985–1.523			
SUV <sub>max</sub> (per 1 unit)	0.920	1.00	0.991–1.008			
Age (per year)	0.159	1.033	0.987–1.080			
Tumor load (per 1 category)	0.015	1.744	1.112–2.736			
Prior treatment lines (1, 2, 3 or more)	0.007	1.488	1.116–1.984	<0.001	1.676	1.258–2.234
Prior chemotherapy (yes vs. no)	0.039	2.031	1.038–3.974			
Log <sub>10</sub> prostate-specific antigen (per 1 unit)	0.476	1.175	0.754–1.829			

**TABLE 4**  
Logistic Regression Analysis for Incomplete <sup>223</sup>Ra Therapy Depending on Multiple Variables

Variable	Univariate regression			Multiple logistic regression		
	P	Hazard ratio	95% CI	P	Hazard ratio	95% CI
%ID (per 1 unit)	0.03	1.059	1.005–1.114			
%ID/L(per 1 unit)	0.029	1.346	1.032–1.757	0.029	1.346	1.032–1.757
SUV <sub>mean</sub> (per 1 unit)	0.158	1.311	0.9–1.910			
SUV <sub>max</sub> (per 1 unit)	0.582	1.003	0.992–1015			
Age (per year)	0.591	1.019	0.95–1.094			
Tumor load (per 1 category)	0.112	1.839	0.867–3.904			
Prior treatment lines (1, 2, 3 or more)	0.927	0.98	0.629–1.525			
Prior chemotherapy (yes vs. no)	0.499	1.44	0.5–4.147			
Log <sub>10</sub> prostate-specific antigen (per 1 unit)	0.238	1.561	0.745–3.268			

omitting any cutoff, our approach does not call for individual adaptation and should be independent of scanner features. Obviously, the presented method does not provide a measure of tumor volume.

Median OS in our cohort was in keeping with the results of the pivotal phase III trial (15.2 vs. 14.9 mo) (10). Compared with the latter, the proportion of patients with extensive bone disease (i.e., more than 20 tumor lesions or a superscan) was considerably higher in the current study (65 vs. 41%). The equal outcome in our study may be due to the availability of treatment options introduced since the previous trial—treatments that may be used after <sup>223</sup>Ra—particularly abiraterone and enzalutamide. In comparison, OS was shorter in the retrospective studies of PET/CT (15) and bone imaging (17). Most probably, this shorter OS might be explained by more advanced tumor burden.

Because mathematic tumor models suggest that <sup>223</sup>Ra targets only a fraction of bone tumor areas (28), there is a need to improve our understanding of <sup>223</sup>Ra distribution. Imaging with <sup>223</sup>Ra for the purpose of dosimetry is limited by the low number of photons (29). It has been shown that uptake of bisphosphonates correlates to that of <sup>223</sup>Ra (30). Though quantitative SPECT/CT cannot be used to clarify the unknown microdistribution, it is obvious that further studies should address individual dosimetry in patients with advanced disease.

Recently, the indication for <sup>223</sup>Ra was restricted by the European Medicines Agency, because in a prospective study the combination of <sup>223</sup>Ra with abiraterone and prednisone or prednisolone was associated with an increased risk for fractures (31). Since no quantitative analysis of bone scans was performed in this study, one can only speculate about the potential influence of bisphosphonate uptake.

Our study had some limitations. It included a relatively small cohort of patients; thus, it has to be considered hypothesis-generating, and a larger study is desirable to confirm the results. However, we could include all patients in the observational period and thus should not expect bias in the selection of our sample. Because of the small absolute number of grade 3–4 cytopenia, our study was not powered to explore the relationship between quantitative imaging parameters and clinically relevant myelosuppression. In the current study, alkaline phosphatase, a potential risk factor for survival in mCRPC patients (32), was not systematically recorded at baseline; thus, it could not be included in the multivariate analysis.

## CONCLUSION

This study indicated that bisphosphonate uptake of the central skeleton as quantified by SPECT/CT before <sup>223</sup>Ra is prognostic of outcome. Our results should encourage further studies on possible prognostic markers including tumor-volume–based quantitation to identify the best approach for risk stratification in mCRPC.

## DISCLOSURE

This study was in part funded by a grant from GE Healthcare to Christian la Fougère. Helmut Dittmann and Christian la Fougère received honoraria from Bayer Pharmaceuticals for advisory boards and training lectures on the use of <sup>223</sup>Ra. No other potential conflict of interest relevant to this article was reported.

## KEY POINTS

**QUESTION:** Is baseline bone scan quantification by SPECT/CT associated with survival in patients starting <sup>223</sup>Ra treatment?

**PERTINENT FINDINGS:** In a prospective clinical cohort study of 60 mCRPC patients assigned for <sup>223</sup>Ra treatment, a high total skeletal bisphosphonate uptake at baseline was associated with significantly shortened survival. Conversely, survival of patients with low uptake was superior to that observed in earlier studies.

**IMPLICATIONS FOR PATIENT CARE:** Quantitative bone scan SPECT/CT may be useful for risk stratification in mCRPC.

## REFERENCES

- Bubendorf L, Schopfer A, Wagner U, et al. Metastatic patterns of prostate cancer: an autopsy study of 1,589 patients. *Hum Pathol.* 2000;31:578–583.
- Riihimäki M, Thomsen H, Brandt A, Sundquist J, Hemminki K. What do prostate cancer patients die of? *Oncologist.* 2011;16:175–181.
- Chandrasekar T, Yang JC, Gao AC, Evans CP. Mechanisms of resistance in castration-resistant prostate cancer (CRPC). *Transl Androl Urol.* 2015;4:365–380.
- Cornford P, Bellmunt J, Bolla M, et al. EAU-ESTRO-SIOG guidelines on prostate cancer. Part II: treatment of relapsing, metastatic, and castration-resistant prostate cancer. *Eur Urol.* 2017;71:630–642.
- Scher HI, Morris MJ, Stadler WM, et al. Trial design and objectives for castration-resistant prostate cancer: updated recommendations from the prostate cancer clinical trials working group 3. *J Clin Oncol.* 2016;34:1402–1418.
- Helyar V, Mohan HK, Barwick T, et al. The added value of multislice SPECT/CT in patients with equivocal bony metastasis from carcinoma of the prostate. *Eur J Nucl Med Mol Imaging.* 2010;37:706–713.

7. Bastawrous S, Bhargava P, Behnia F, Djang DS, Haseley DR. Newer PET application with an old tracer: role of  $^{18}\text{F}$ -NaF skeletal PET/CT in oncologic practice. *Radiographics*. 2014;34:1295–1316.
8. Mohler JL, Armstrong AJ, Bahnson RR, et al. Prostate cancer, version 1.2016. *J Natl Compr Canc Netw*. 2016;14:19–30.
9. Goyal J, Antonarakis ES. Bone-targeting radiopharmaceuticals for the treatment of prostate cancer with bone metastases. *Cancer Lett*. 2012;323:135–146.
10. Parker C, Nilsson S, Heinrich D, et al. Alpha emitter radium-223 and survival in metastatic prostate cancer. *N Engl J Med*. 2013;369:213–223.
11. Sartor O, Coleman R, Nilsson S, et al. Effect of radium-223 dichloride on symptomatic skeletal events in patients with castration-resistant prostate cancer and bone metastases: results from a phase 3, double-blind, randomised trial. *Lancet Oncol*. 2014;15:738–746.
12. Jacene H, Gomella L, Yu EY, Rohren EM. Hematologic toxicity from radium-223 therapy for bone metastases in castration-resistant prostate cancer: risk factors and practical considerations. *Clin Genitourin Cancer*. 2018;16:e919–e926.
13. Den RB, George D, Pieczonka C, McNamara M. Ra-223 treatment for bone metastases in castrate-resistant prostate cancer: practical management issues for patient selection. *Am J Clin Oncol*. 2019;42:399–406.
14. Vogelzang NJ, Coleman RE, Michalski JM, et al. Hematologic safety of radium-223 dichloride: baseline prognostic factors associated with myelosuppression in the ALSYMPCA trial. *Clin Genitourin Cancer*. 2017;15:42–52.e8.
15. Etchebehere EC, Araujo JC, Fox PS, Swanston NM, Macapinlac HA, Rohren EM. Prognostic factors in patients treated with  $^{223}\text{Ra}$ : the role of skeletal tumor burden on baseline  $^{18}\text{F}$ -fluoride PET/CT in predicting overall survival. *J Nucl Med*. 2015;56:1177–1184.
16. Ulmert D, Kaboteh R, Fox JJ, et al. A novel automated platform for quantifying the extent of skeletal tumour involvement in prostate cancer patients using the bone scan index. *Eur Urol*. 2012;62:78–84.
17. Fosbøl MØ, Petersen PM, Kjaer A, Mortensen J.  $^{223}\text{Ra}$  therapy of advanced metastatic castration-resistant prostate cancer: quantitative assessment of skeletal tumor burden for prognostication of clinical outcome and hematologic toxicity. *J Nucl Med*. 2018;59:596–602.
18. Agrawal K, Marafi F, Gnanasegaran G, Van der Wall H, Fogelman I. Pitfalls and limitations of radionuclide planar and hybrid bone imaging. *Semin Nucl Med*. 2015;45:347–372.
19. Constable AR, Cranage RW. Recognition of the superscan in prostatic bone scintigraphy. *Br J Radiol*. 1981;54:122–125.
20. Bailey DL, Willows KP. Quantitative SPECT/CT: SPECT joins PET as a quantitative imaging modality. *Eur J Nucl Med Mol Imaging*. 2014;41(suppl 1):S17–S25.
21. Bailey DL, Willows KP. An evidence-based review of quantitative SPECT imaging and potential clinical applications. *J Nucl Med*. 2013;54:83–89.
22. Home page. DRKS: German Clinical Trials Register website. <https://www.drks.de>. Updated July 31, 2020. Accessed August 5, 2020.
23. CTCAE files. National Cancer Institute Enterprise Vocabulary Services website. <https://evs.nci.nih.gov/ftp1/CTCAE/About.html>. Accessed August 5, 2020.
24. Umeda T, Koizumi M, Fukai S, et al. Evaluation of bone metastatic burden by bone SPECT/CT in metastatic prostate cancer patients: defining threshold value for total bone uptake and assessment in radium-223 treated patients. *Ann Nucl Med*. 2018;32:105–113.
25. Arvola S, Jambor I, Kuisma A, et al. Comparison of standardized uptake values between  $^{99\text{m}}\text{Tc}$ -HDP SPECT/CT and  $^{18}\text{F}$ -NaF PET/CT in bone metastases of breast and prostate cancer. *EJNMMI Res*. 2019;9:6.
26. Kuji I, Yamane T, Seto A, Yasumizu Y, Shirotake S, Oyama M. Skeletal standardized uptake values obtained by quantitative SPECT/CT as an osteoblastic biomarker for the discrimination of active bone metastasis in prostate cancer. *Eur J Hybrid Imaging*. 2017;1:2.
27. Matheoud R, Goertzen AL, Vigna L, Ducharme J, Sacchetti G, Brambilla M. Five-year experience of quality control for a 3D LSO-based whole-body PET scanner: results and considerations. *Phys Med*. 2012;28:210–220.
28. Moreira HMR, Guerra Liberal FDC, O'Sullivan JM, McMahon SJ, Prise KM. Mechanistic modeling of radium-223 treatment of bone metastases. *Int J Radiat Oncol Biol Phys*. 2019;103:1221–1230.
29. Hindorf C, Chittenden S, Aksnes AK, Parker C, Flux GD. Quantitative imaging of  $^{223}\text{Ra}$ -chloride (Alpharadin) for targeted alpha-emitting radionuclide therapy of bone metastases. *Nucl Med Commun*. 2012;33:726–732.
30. Pacilio M, Ventroni G, De Vincentis G, et al. Dosimetry of bone metastases in targeted radionuclide therapy with alpha-emitting  $^{223}\text{Ra}$ -dichloride. *Eur J Nucl Med Mol Imaging*. 2016;43:21–33.
31. Smith M, Parker C, Saad F, et al. Addition of radium-223 to abiraterone acetate and prednisone or prednisolone in patients with castration-resistant prostate cancer and bone metastases (ERA 223): a randomised, double-blind, placebo-controlled, phase 3 trial. *Lancet Oncol*. 2019;20:408–419.
32. Pinart M, Kunath F, Lieb V, Tsaor I, Wullich B, Schmidt S; German Prostate Cancer Consortium (DPKK). Prognostic models for predicting overall survival in metastatic castration-resistant prostate cancer: a systematic review. *World J Urol*. 2020;38:613–635.